Original Article

Liver Tissue Bioengineering: Decellularization and Recellularization. Histological and Immunohistochemical Study

Shaimaa Fattin Khedr, Nagwa Kostandy Kalleny and Nevert Farid Abd ELSalam

Department of Histology and Cell Biology, Faculty of Medicine, Ain Shams University, Cairo, Egypt

ABSTRACT

Introduction: The need for liver transplantation is rising due to increase in end-stage liver diseases. Testing drug toxicity on either liver tissue or on adult hepatocytes is crucial as it is the major drug metabolizing organ.

Aim of the Work: This study aimed to form natural liver scaffold by decellularization followed by recellularization using adult male albino rat hepatocytes to form auxiliary hepatic tissue, and to culture adult hepatocytes for experimental studies and liver bioengineering.

Material and Methods: Group I: [10 rats] control group. Group II: [10 rats] liver decellularization group. Group III: [20 rats] 10 rats used as adult hepatocyte donor for recellularization, and some hepatocytes were cultivated in culture flasks to ensure proliferation, while another 10 rats' livers were decellularized followed by liver recellularization. At the end of the experiment, livers of control, decellularized scaffold, and recellularized tissue were processed for histological, histochemical and immunohistochemical techniques. Morphometrical and statistical studies were also performed.

Results: Grossly, decellularized livers appeared semi-transparent. Histologically they appeared as an acellular liver matrix with apparently preserved hepatic architecture. The cultivated hepatocytes in culture flasks showed progressively increased number till confluency at day 21. They appeared polygonal with granular cytoplasm when cocultured with other cells. Recellularized livers showed hepatocyte aggregations with satisfactory preservation of extracellular matrix. Reseeded hepatocytes appeared polygonal with acidophilic, granular and Periodic acid-Schiff positive cytoplasm. Also, they showed significant increase in mean number of cells exhibiting positive reaction for proliferating cell nuclear antigen and Alpha-fetoprotein immune-stained sections compared to control.

Conclusion: Cultivated adult rat hepatocytes proliferated till confluency in culture flasks. Well-structured decellularized tissue was formed that supported hepatocyte survival and proliferation, thus, this recellularized liver model and the cultured hepatocytes can be used for pharmaceutical testing on liver models and could be a new hope for patients with liver diseases.

Received: 22 March 2022, **Accepted:** 31 March 2022

Key Words: Bioengineering, decellularization, histological, liver, recellularization.

Corresponding Author: Shaimaa Fattin Khedr, PhD, Department of Histology and Cell Biology, Faculty of Medicine, Ain Shams University, Cairo, Egypt, **Tel.**: +20 10 1248 2252, **E-mail:** shaimaafattin@gmail.com

ISSN: 1110-0559, Vol. 46, No. 3

INTRODUCTION

Liver diseases are rising worldwide creating a global health burden. Deaths due to different liver diseases in Egypt reached 10.45% of total deaths according to World Health Organization (WHO) published data in 2017[1]. Liver transplantation is the last line of treatment for end stage liver diseases (ESLD). Nevertheless, available donor livers for transplantation are scarce and the recipient will face the drawbacks of long term use of immunosuppressant after successful transplantation[2]. Moreover, liver transplantation remains limited due to suboptimal long-term outcomes. An innovative generation of therapeutics which target hepatocytes could sidestep the need for liver transplantation in cirrhotic and ESLD patients[3]. Hepatocytes have a remarkable capacity for regeneration. Thus, hepatocyte transplantation (HT) was considered as a good treatment alternative to liver transplantation[4].

In addition, experimental studies on animals which target the effect of different drugs [pharmaceutical testing], toxins, nutrients on the liver tissue and disease modeling are growing rapidly because of the increased diversity in these fields[5]. Therefore, creating an in-vitro hepatic model tailored for experimental studies would save money and lives of many experimental animals and could give detailed results equivalent to in *vivo* studies[6].

Moreover, whole organ decellularization and recellularization is considered a promising modality for treatment of ESLD and for performing experimental studies. Decellularization is the process of removal of parenchymatous and non-parenchymatous cells from the surrounding stroma of the donor organ producing a three-dimensional [3D] scaffold that has the same ultra-structure and vascular networks for gas and nutrient exchange[7].

Extracellular matrix not only provides a 3D mechanical support to maintain tissue and organ structure, but it also creates microenvironment by providing biochemical cues and structural information to the inhabiting cells[8,9]. Despite unavoidable degree of ECM disruption during

 DOI: 10.21608/ejh.2022.128857.1664

decellularization, it still have a complex reservoir for growth factors and cytokines that are effective to robust cell growth[10,11].

For recellularization, the decellularized liver matrix [DLM] will need much lower cell count than native liver to perform normal physiological function[12]. Therefore, cells isolated from one donor can be harvested for multiple patients and the remaining cells can be cryopreserved for later use[13]. Therefore, primary adult hepatocytes [AdH] are ideal for liver bioengineering due to its adequate proliferative capacity[14].

AIM OF THE WORK

This study aimed to form natural liver scaffold by decellularization followed by recellularization using adult male albino rat hepatocytes to form auxiliary hepatic tissue, and to culture adult hepatocytes for experimental studies and liver bioengineering.

MATERIALS AND METHODS

Experimental Animals

This experiment was conducted on forty adult male albino rats of average weight of 170 gram (gm), which were purchased from the animal house of Medical Ain Shams Research Institution (MASRI). They were used for liver harvesting and the preparation of the 3D liver scaffold (decellularized tissue) as well as obtaining donor adult hepatocytes for recellularization and also for in vitro culturing in culture media flasks. This research was performed in the MASRI, Faculty of Medicine, Ain Shams University and in the Stem Cell Research Lab, Histology and Cell Biology Department, Faculty of Medicine, Ain Shams University. All animal procedures were performed in accordance with the general guidelines for the care and use of laboratory animals and approved by the Animal Ethical Committee, Faculty of Medicine, Ain Shams University.

Animal Groups

In the present study the animals were divided into three main groups.

Group I [control group]: consists of 10 adult male albino rats, to study normal histological structure of the adult rat liver.

Group II [decellularization group]: consists of 10 adult male albino rats whose livers were decellularized[15].

Group III [recellularization group]: consists of 20 rats in which 10 adult male albino rats were considered donors for recellularization by AdHs, and also other isolated adult hepatocytes were cultured in vitro to check the proliferative capacity of the cells. Another 10 adult male albino rats' livers were subjected to decellularization process followed by recellularization using the donor AdH[15].

Liver harvest operation for decellularization[12,16]

Each rat was heparinized and anesthetized using thiopental sodium 30 milligram (mg)/ kilogram (kg) intraperitoneal injection[17]. For sterilizing the rat's abdominal and thoracic area, swabbing by sterile dressing soaked with 70% alcohol was done. A midaxillary surgical incision was made through the skin followed by cutting the muscle layer to visualize the abdomen as well as the thorax. The stomach and bowel were moved to the left side and ligaments attached liver to stomach and spleen were carefully cut. The diaphragm was incised, and the aorta was transected. The hilum of liver and its blood vessels were visualized. Portal vein (PV) was cut at the nearest point to the intestine. Livers were then collected, and each was laid in sterile petri-dish preparing for its cannulation. The PV was cannulated by a 24-gauge cannula and secured by two 4.0 silk stitches. Each liver was perfused with calcium-magnesium free phosphate buffer saline (CMF-PBS) (manufactured by PAN Biotech) to ensure cannula position (Figures 1a,b). Then, each liver was weighted in the sterile petri-dish with the cannula and the two 4.0 silk sutures (wt. a). Finally, the liver was frozen at -80 oC in a cell culture dish with CMF-PBS till decellularization.

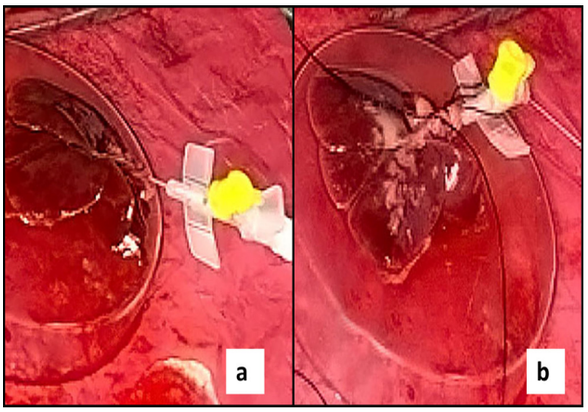

Fig. 1: A photograph of: a- a cannulated adult albino rat liver. b- liver after CMF-PBS perfusion to ensure cannula position in the PV.

Whole liver decellularization Procedure

It was done according to some previous studies[12,15] with some modification according to the pilot study. Whole liver decellularization procedures were accomplished at the Stem Cell Research Lab, Histology and Cell Biology Department, Faculty of Medicine, Ain Shams University.

Initial physical decellularization was done by freezing at -80oC for 48 hours (hrs) followed by thawing to room temperature. After thawing, the cannulated livers were weighted to calculate its weight after freezing (wt. b).

Decellularization by chemical methods was done by putting the liver in sterile glass petri-dish at room temperature. Then, the cannula was connected to a sterile intravenous (IV) line to a 50 milliliter (ml) syringe attached to a syringe pump. First, distilled water (DW) was perfused

in the cannula to remove residual blood at a rate of 1 ml/minute [min] for 2-3 hrs till a clear fluid appeared coming out of the liver. Then, 0.5% sodium dodecyl sulfate (SDS) infusion for 6-8 hrs was performed until the liver appeared white. The infusion rate started at 2 ml/min till reaching 6-8 ml/min. Washing with DW was done to remove SDS at a rate of 6-8 ml/min for 1 hr, followed by1% Triton X-100 infusion for 3 hrs at a rate of 6-8 ml/min to ensure complete decellularization. Finally, washing with DW was performed for 3-4 hrs at a rate of 6-8 ml/min to remove any residual chemicals from DLM. Whereas, for DLM that was going to undergo recellularization, final wash with CMF-PBS with penicillin/streptomycin for 1 hr was performed. Then, it was stored in the fridge at 4oC temperature for 2-3 days.

The DLM was weighted after complete decellularization (wt. c) to be compared with the liver weight before freeze/thaw cycle (wt. a), and after freeze/thaw cycle (wt. b). The weight of cannula, the same length of two 4.0 silk sutures and the empty petri-dish were reduced from (wt. a), (wt. b), (wt. c) to calculate the net weight of the liver. Finally, the right lobe of DLM underwent regular procedures of histological, histochemical, immunohistochemical, morphometric and statistical studies.

Isolation of adult rat hepatocytes [AdH]

It was done according to some previous studies[12,18] with some modification according to the pilot study. Primary AdHs were obtained from apparently normal liver tissue of adult male albino rats. Each liver was excised under complete aseptic conditions (similar to the excision of livers used for decellularization process) under anesthesia using thiopental sodium 30 mg/kg intraperitoneal injection[17]. Each liver was put in cold CMF-PBS and was quickly transported in an ice box to the Stem Cell Research Unit. Then, each liver was rinsed three times in cold CMF-PBS with penicillin/streptomycin in a sterile glass beaker and then put in a sterile petri-dish in the laminar air flow. It was minced into 1-5 mm pieces by a sterile scalpel. Liver pieces were added to 10 ml tissue digestion solution [type I collagenase 0.1% manufactured by Sigma-Aldrich] in a 50 ml falcon tube, then the falcon tube was put in a shaking water bath at 37oC for 30 min, to ensure optimal collagenase activity. Then, 200-250 ml of CMF-PBS was added gradually to the digested liver pieces and the mixture was filtered through Sigma stainless mesh into a sterile glass container. The filtrate was centrifuged at 1000 round per min, for 5 min, at 4oC to obtain the cell pellet. The supernatant containing most of the non-parenchymatous cells was discarded. Centrifugation and pellet collection steps were repeated twice. Meanwhile, hepatocyte complete media (HCM) was formed from 88.2% Dulbecco's Modified Eagle Medium with Ham's F-12 (DMEM F-12) (manufactured by Lonza.), 10% fetal bovine serum (FBS) (manufactured by PAN Biotech), 1% of penicillin, streptomycin, and amphotericin B (manufactured by PAN Biotech), 7.5 microgram (ug)/ml hydrocortisone (manufactured by Pfizer), 0.5 IU/ml Insulin (manufactured by Novo Nordisk), and 0.3 nanogram (ng)/ml epidermal growth factor (EGF) (manufactured by Elabscience). Finally, HCM was added to the final cell pellet. Cell count and viability were measured using manual hemocytometer. A 50 microliter [ul] of cell suspension was mixed with 50 ul of trypan blue stain to examine hepatocytes viability by staining dead cells[19]. Trypan blue stain enters the cells with defective plasma membrane giving dark blue color. Whereas, normal cells with intact cell membrane are impermeable to staining with trypan blue thus they appear pale/colorless[20].

The number of hepatocytes (Total or viable) is calculated as follows

Yield [counted cells] = total or viable cells counted in large squares/number of large squares counted x 2 x 10,000 x volume of cell suspension in ml.

The viability of hepatocytes is calculated as follows

Percentage of viable hepatocytes [%] = number of viable cells [pale/colorless cells] x 100/total number of cells.

Cultivation of adult hepatocytes[21,22]

Hepatocytes were seeded at a concentration of 4 x 10^6 in 2 ml HCM into 75 ml culture media flask. Culture media flasks were put in the incubator for an attachment period of 2 hrs. After the attachment period, the flasks were washed twice with PBS and 10 ml HCM was added. Then, the flasks were checked every other day for follow up, noticing cell adherence to the culture flask, ensuring absence of infection, and determining proliferation via noticing the apparent increase in number of cultured adult hepatocytes and their confluency. The media was changed twice a week till reaching confluency.

Recellularization of decellularized liver matrix

Decellularized liver matrix sterilization and preparation

It was done according to some previous studies[12,23] with some modification according to the pilot study. The DLM was allocated to a new sterile petri-dish. Firstly, the DLM was perfused with 70% ethanol via PV for 30 min, followed by perfusion with CMF-PBS containing 1% penicillin, streptomycin and amphotericin B for 1 hr at a rate of 4 ml/min Then, the DLM was transferred to the laminar air flow and ultraviolet (UV) light was used for 20 min on each side of the scaffold. Finally, it was connected to the perfusion system for 24 hrs pumping HCM at a rate of 2 ml/hr for preparation before introducing adult donor hepatocytes.

Recellularization using adult hepatocytes

It was done according to previous studies[12,15] with some modification according to the pilot study. Isolated primary AdH obtained from donor adult male albino rat liver were diluted in HCM to be adjusted at 2 x10^6 cell/ml HCM. A total of 20-40 x106 cells were introduced

slowly manually into the whole DLM through PV vein 1 ml every 5 min. It was observed that the DLM color changed gradually, and its blood vessels appeared opaque due to the reseeded AdH (Figure 2). The recellularized liver was transferred to an incubator for 3-6 hrs for static culture. Finally, the cannula in the recellularized liver was connected via a sterile IV line to a perfusion syringe pump [hawkmed® HK-400II syringe pump by Shenzhen Hawk Optical Electronic Instrument CO., LTD.]. During the recellularization procedure, the liver was perfused by HCM at a rate of 2 ml/hr for 5 days. The whole liver appeared opaque compared to day 1 (Figure 3).

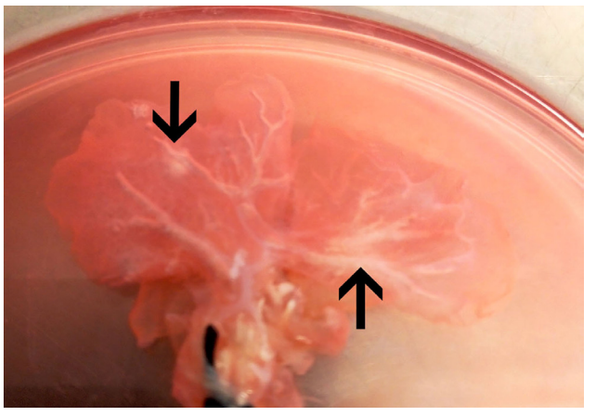

Fig. 2: A photograph showing gross picture of the recellularized scaffold of adult male albino rat liver in day 1 after reseeding of AdH. The blood vasculature appears opaque (→).

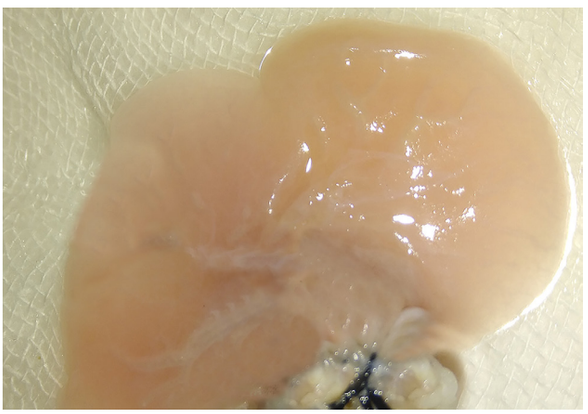

Fig. 3: A photograph showing gross picture of the recellularized scaffold of adult male albino rat in day 5 after reseeding of AdH. The whole liver appears opaque compared to recellularized scaffold of day 1.

Histological, histochemical and immunohistochemical Methods

Specimens from the right lobe of the livers from each animal were fixed in 10% formalin solution for one week. Then, dehydration, clearing, impregnation in soft paraffin and finally embedding in hard paraffin to form paraffin blocks. Serial sections were cut at 4-5 µm thickness and subjected to the following techniques: Hematoxylin and Eosin stain [H&E] to evaluate general structure preservation and complete removal of cellular debris [15]. Mallory stain to evaluate the integrity of collagen fibers in the matrix[24]. Periodic acid Schiff [PAS] reaction counter stained with Haematoxylin [Hx] technique to evaluate the integrity of glycoprotein (GP) and proteoglycan (PG) in ECM and the intrahepatic glycogen content[25]. Moreover, proliferating cell nuclear antigen [PCNA] (Primary antibody; anti-PCNA, mouse anti-rat monoclonal, Dako. Secondary antibody; Goat anti-mouse polyclonal, Jackson ImmunoResearch) indirect immunohistological staining was used to identify proliferating cells in the tissue section. The PCNA immunohistochemistry positive reaction appeared as brown color in the nuclei of the hepatocytes demarcating their proliferation[26]. Alpha Fetoprotein [AFP] (Primary antibody Anti-AFP, rabbit anti-rat polyclonal, Prosci. Secondary antibody: Goat anti-rabbit polyclonal, Jackson ImmunoResearch) indirect immunohistological staining was used to verify the cell origin. The AFP immunohistochemistry positive reaction appeared as brown color in the cytoplasm of the hepatocytes demarcating the cell origin[27].

Morphometric and statistical studies

Histological, histochemical and immune-stained slides were examined using Leica Q500 MC program in the Histology Department, Faculty of Medicine, Ain Shams University. The computer was connected to an Olympus XB microscope- Japan. The measurements were done per high power field [x400] in ten random non overlapping fields in each of ten stained sections obtained from ten animals in each group for each of the following morphometric measures:

Measuring mean area percentage of collagen using Mallory-stained sections of all studied groups.

Measuring mean optical density of Extracellular GP, PG and reticular fibers [positive PAS reaction in ECM] using PAS counter stained with Hx sections of all studied groups.

Measuring the mean optical density of glycogen in hepatocytes [positive PAS reaction inside hepatocytes] using PAS counter stained with Hx sections of control and recellularized groups.

Measuring the mean number of PCNA positive hepatocytes in the control and recellularized groups.

Measuring the mean number of AFP positive hepatocytes in the control and recellularized groups.

Statistical analysis

The mean liver weight and the mean of the morphometric measured parameters recorded for each group were calculated and the data were presented as mean ± standard deviation (SD). Statistical analysis was carried out using statistical package for the social sciences [SPSS], software program, version 20 [IBM corporation, Armwork, North castle, Westchesten Country, New York, USA].

Statistical difference among groups for each parameter was determined using one-way analysis of variance [ANOVA] followed by post hoc least significance difference [LSD] for comparison between more than two groups. If the probability *p value* ≤ 0.05, then the differences were considered statistically significant.

RESULTS

Gross results of decellularized liver

The decellularization process was done successfully for each of the 10 rats of group II (decellularization group). A white partially transparent liver was obtained after complete liver decellularization process which lasted for 15-19 hrs (Figure 4). The mean weight of livers in group II before freezing (wt a) measured 15.96 ± 2.06 gm, after freezing/thawing (wt b) measured 15.53 ± 2.01 gm and after complete decellularization (wt c) measured 5.11 ± 0.77 gm (Table 1). The mean liver weight of the completely decellularized livers was significantly decreased (*p value* ≤ 0.05) as compared to the mean liver weight before and after its freezing/thawing (Histogram 1).

The morphology of the primary culture of adult rat hepatocytes by the phase contrast microscope

Sample of AdH cell pellet was stained with trypan blue and examined using phase contrast microscope in day zero using hemocytometer. Examination of AdH revealed rounded to polygonal suspended cells. Hepatocytes usually showed single nucleus; however, some hepatocytes were binucleated (Figure 5). Mean number of isolated viable AdH cell count (C1) and total AdH cell count (C2) were measured and the percentage of viable cells (%) was calculated (Table 2). Mean number of viable cells measured was 4.46 x108 cells and their viability was 91.39%.

By the low power the cultivated AdH showed apparent progressive increase in number of attached cells throughout the culturing time. On day two, the polygonal AdH appeared scattered with few ellipsoid cells in between (Figure 6). On day seven, both AdH and ellipsoid cells were apparently increased in number and were in close proximity to each other (Figure 7). On day fourteen, AdH showed 50 – 75% confluency (Figure 8). Finally, on day twenty-one AdH became almost 90-95% confluent (Figure 9). Whereas, by high power throughout the days of cultivation, AdHs appeared polygonal in shape with granular cytoplasm and their cell membrane showed a hallo around the cell. Signs of mitosis were seen in some AdH especially on day seven and day fourteen. Other spindle/star shaped cells were seen in close proximity with many hepatocytes (Figures 10–13). On day two, cells were scattered either individually or in form of two cells close together (Figure 10). On day seven, AdH mostly formed cords of three or more cells (Figure 11). On day fourteen, AdH appeared formed of single or double cell cords of more than three cells (Figure 12). On day twenty-one, AdH formed long single or double cell cords. Cells at some areas appeared overlapping each other (Figure 13).

Histological, histochemical, immunohistochemical, morphometric, and statistical results of experimental groups

Histological results

The H&E-stained sections of group I [control group] showed hardly delineated hepatic lobules that showed central veins and peripheral portal tracts and surrounded by liver capsule. Cords of hepatocytes appeared branching and anastomosing radiating from the central vein and were separated by blood sinusoids (Figure 14). Each hepatocyte appeared as an acidophilic polygonal cell having rounded central single or double vesicular nuclei. Portal tract was identified at the corners of the lobules. They were formed of stroma of connective tissue containing a branch from hepatic artery, PV, and bile ductule (Figure 15).

Group II [decellularization group] showed that the general architecture of the decellularized liver was almost preserved, however, it appeared collapsed on itself with apparent decreased distance between portal tracts as compared with control group. Delicate liver stroma was seen with complete loss of parenchymal and non-parenchymal cells in the DLM (Figure 16). Portal tract could be identified as an area with few empty spaces showing condensed collagen fibers that demarcated the decellularized hepatic artery, PV and bile ductule (Figure 17).

Group III [recellularization group] showed acidophilic collagen fibers in the recellularized hepatic tissue that contained few AdH in the matrix and some aggregations of reseeded AdH appeared inside PV branches (Figure 18). The aggregated reseeded AdH appeared polygonal in shape that formed cords of hepatocytes. The hepatocytes showed acidophilic granular cytoplasm and rounded central nucleus (Figure 19).

Mallory-stained sections for group I [control group] showed collagen fibers condensed around structures in the portal area (Figure 20). In Group II [decellularization group] collagen fibers were seen in the DLM, moreover they showed condensation around large vessels and structures in the portal tract (Figure 21). Group III [Recellularization group] showed collagen fibers in the liver capsule and in the recellularized liver matrix. The collagen fibers appeared condensed around large blood vessels. Large polygonal cells resembling hepatocytes were seen inside a portal branch. Some cells appeared infiltrating the liver matrix (Figure 22). Statistical analysis of mean area percentage of collagen showed insignificant difference ($p > 0.05$) between control group (9.2 ± 1.5), decellularization group (10.4 ± 2.3), and recellularization group (11.4 ± 3.3) (Histogram 2).

Histochemical results

The PAS-stained sections for group I [control group] showed that the hepatocytes contained PAS positive cytoplasmic granules, also the surrounding ECM exhibited PAS positive reaction (Figure 23). Group II [decellularization group] showed well-defined PAS positive reaction of GPs,

PGs and reticular fibers in the DLM (Figure 24). Group III [recellularization group] showed that the hepatocytes exhibited intense PAS positive cytoplasmic reaction. The remaining matrix of recellularized tissue exhibited PAS positive reaction (Figure 25). Statistical analysis of the mean optical density of GPs, PGs and reticular fibers in the ECM showed statistically insignificant difference ($p > 0.05$) between control group (68.2 ± 9.6), decellularization group (69.6 ± 3.7), and recellularization group (64.5 ± 4.3) (Histogram 3). However, the mean optical density of intrahepatic glycogen was significantly increased (p *value* ≤ 0.05) in the recellularization group (78.9 ± 1.9) compared with the control group (72.9 ± 3.0) (Histogram 4).

Immunohistochemical results

The PCNA immuno-stained sections of group I [control group] exhibited brown color of positive PCNA nuclear reaction in cells near the portal area especially those lining bile duct more than other areas of hepatic lobule. Few hepatocytes exhibited positive PCNA nuclear reaction (Figure 26). Group II [decellularization group] showed negative PCNA nuclear reaction (Figure 27). Group III [Recellularization group] exhibited brown color of positive PCNA nuclear reaction in the recellularized hepatocytes that were present inside a PV (Figure 28). Statistical analysis revealed that there was significant increase ($p \leq 0.05$) in the mean number of hepatocytes with PCNA positive nuclear reaction in group III (6.2 ± 2.0) in comparison to group I (3.0 ± 0.8) [Histogram 5].

The AFP immuno-stained sections of group I [control group] exhibited brown color of positive AFP cytoplasmic reaction in few hepatocytes (Figure 29). Group II [decellularization group] showed negative cytoplasmic reaction for AFP (Figure 30). Group III [Recellularization group] exhibited brown color of positive reaction in the cytoplasm of most of the reseeded hepatocytes (Figure 31). Statistical analysis revealed significant increase ($p \leq 0.05$) in the mean number of hepatocytes with AFP positive cytoplasmic reaction in group III (7.4 ± 1.0) in comparison to group I (2 ± 0.5) [Histogram 6].

Fig. 4: A photograph showing gross picture of adult male albino rat liver after complete decellularization process. The liver appears semi-transparent. The hepatic vasculature is apparently seen as white branches.

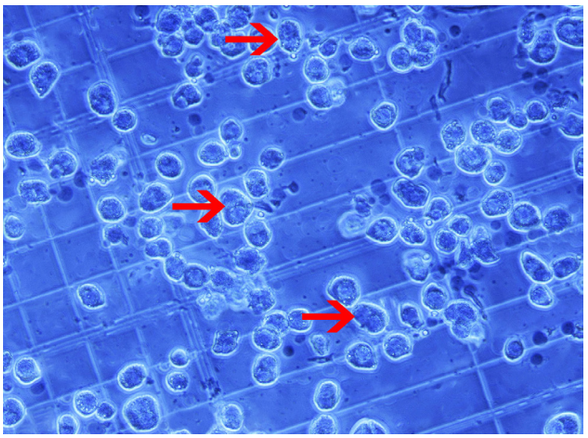

Fig. 5: Showing AdH on day zero on hemocytometer. Hepatocytes appear polygonal or rounded cells. Cells have single nucleus and others were binucleated (→). (Phase contrast, Trypan blue x 400)

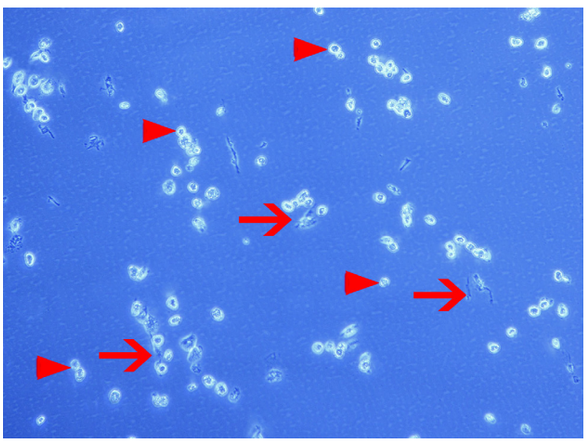

Fig 6: Showing AdH on day two. Polygonal cells (AdH) appear adherent to the flask (►). They are scattered in the culturing flask with few ellipsoid cells in between (→). (Phase contrast photomicrograph, x 100)

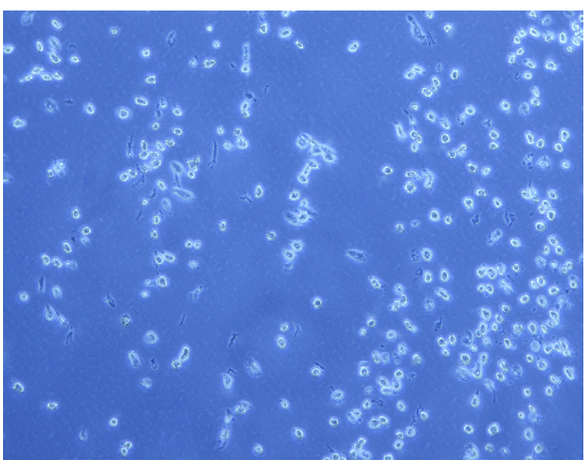

Fig. 7: Showing AdH on day seven, hepatocytes number is apparently increased. Ellipsoid cells are apparently increased in number and found in close relation to hepatocytes. (Phase contrast, x 100)

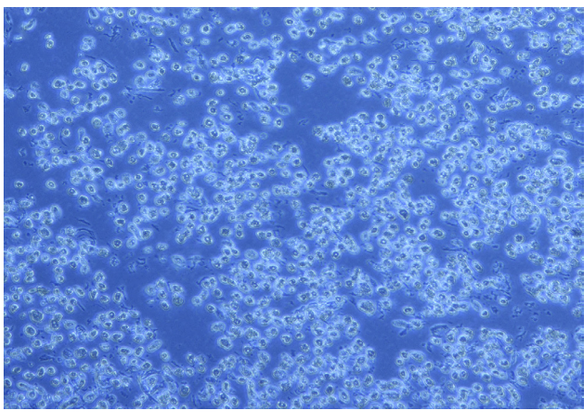

Fig 8: Showing AdH on day fourteen of the culture. Increase in number of hepatocytes with 50 – 75% confluence is apparent (compared to day seven). (Phase contrast photomicrograph, x 100)

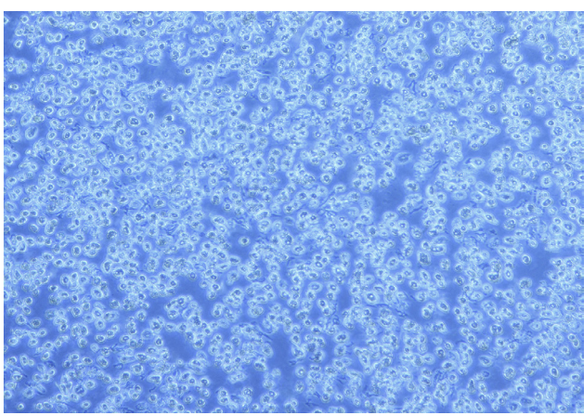

Fig. 9: Showing AdH on day twenty-one. Cells are mostly confluent (about 90-95%). (Phase contrast photomicrograph, x 100)

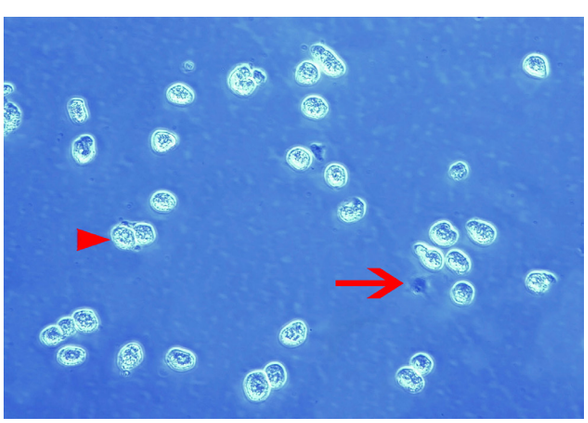

Fig 10: Showing AdH (►) on day two. They are polygonal in shape with granular cytoplasm and their cell membranes form a hallo around the cells. Cells were scattered either individually or in form of two cells close together. Few ellipsoid/star shaped cells are seen in close contact with AdHs (→). (Phase contrast photomicrograph, x 400)

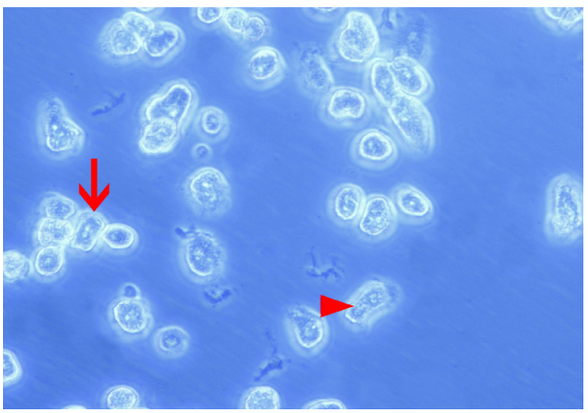

Fig. 11: Showing AdH on day seven. Signs of mitosis could be seen most probably in telophase. Cultured hepatocytes appear as polygonal cells with single nucleus and others are binucleated (►). The cells mostly form cords of three or more cells (→). (Phase contrast photomicrograph, x 400)

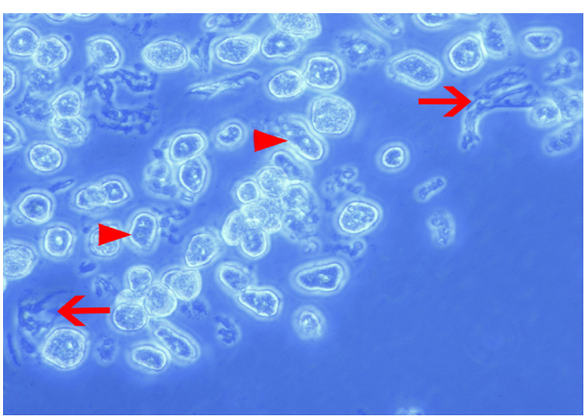

Fig 12: Showing AdH on day fourteen. Cells have single or double nuclei, granular cytoplasm, and bright cell membrane. Signs of mitosis mostly in telophase can be seen in some hepatocytes (►). They formed single or double cell cords mostly of multiple cells. Other star shaped cells (→) are seen in between hepatocytes. Other cells showed multiple processes joining many hepatocytes. (Phase contrast photomicrograph, x 400)

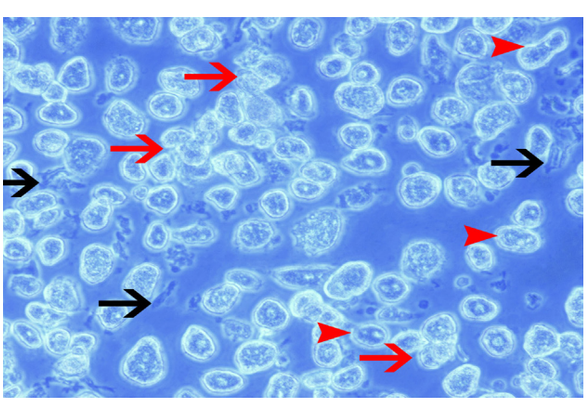

Fig. 13: Showing AdH on day twenty-one. Cells have one or two nuclei with granular cytoplasm. Mitotic figures can be seen in some cells (►). They create long single or double cell cords. Spindle shaped cells can be seen in between (black arrow). Cells at some areas form multiple layers (red arrow). (Phase contrast photomicrograph, x400)

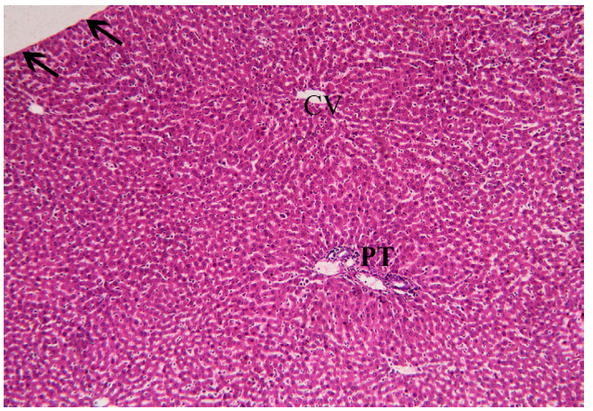

Fig. 14: A photomicrograph of an adult male albino rat liver of the control group showing classic hepatic lobule with ill-defined boundaries. Notice central veins (CV), a portal tract (PT) and liver capsule (→) are seen. (H&E x100)

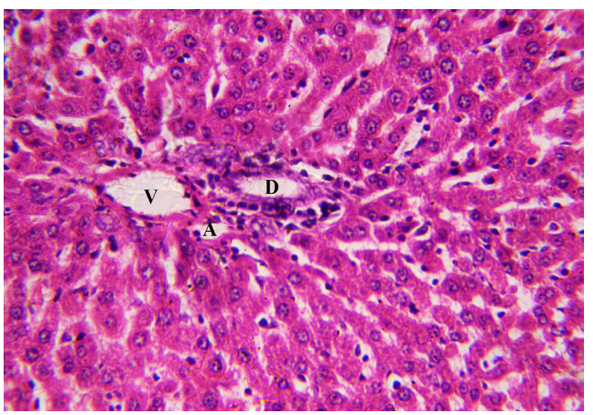

Fig. 15: A photomicrograph of an adult male albino rat liver of the control group showing the portal tract having a branch of hepatic artery (A), a portal venule (V) and a bile ductule (D). (H&E x400)

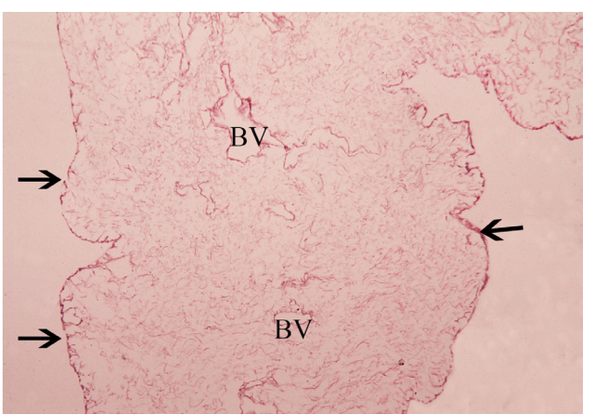

Fig. 16: A photomicrograph of a section in DLM of group II (decellularization group) showing preservation of the hepatic architecture with acellular a matrix. Large blood vessels can be seen (BV). Intact hepatic capsule (→) can be seen surrounding the liver tissue. (H&E x100)

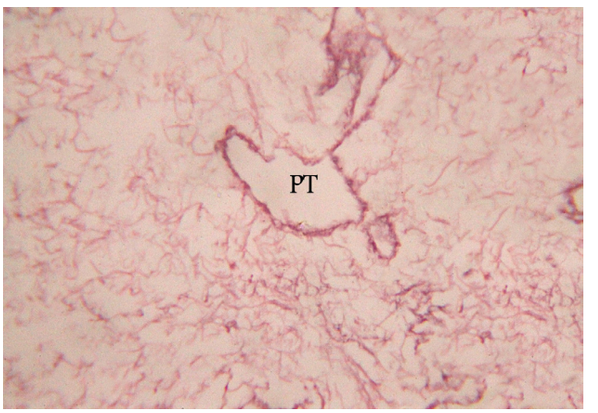

Fig. 17: A photomicrograph of a DLM of group II (decellularization group) showing the portal tract surrounded by an acellular matrix. The PV, hepatic artery and bile duct cannot be precisely identified. (H&E x400)

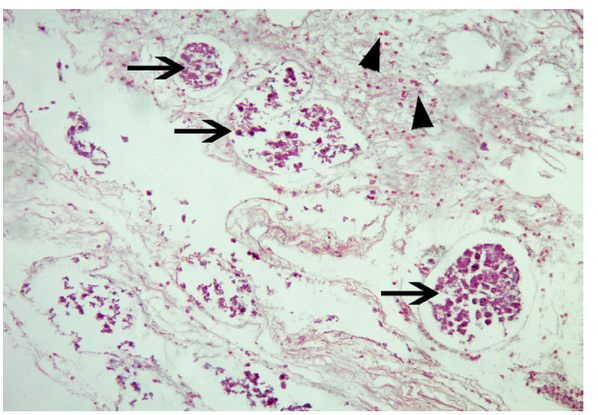

Fig. 18: A photomicrograph of a section in recellularized scaffold of group III showing aggregation of reseeded cells in PV branches (→). Some cells are present in the remaining matrix of the recellularized scaffold (►). Notice acidophilic collagen fibers in the recellularized scaffold. (H&E, x100)

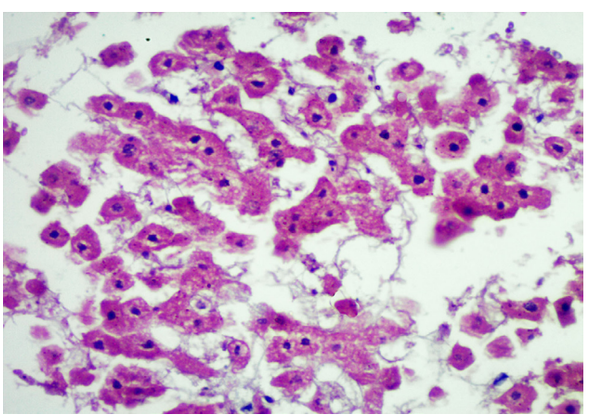

Fig. 19: A photomicrograph of a recellularized scaffold of the group III showing an aggregation of hepatocytes forming cords of reseeded hepatocytes separated by spaces. Collagen fibers are seen in-between the cells. (H&E x400)

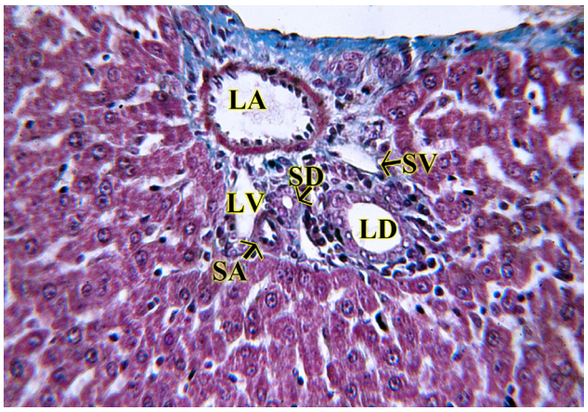

Fig. 20: A photomicrograph of an adult male albino rat liver of the control group showing some collagen fibers surrounding large bile duct (LD), small bile duct (SD), large artery (LA), small artery (SA), large vein (LV) and small vein (SV). (Mallory stain, x400)

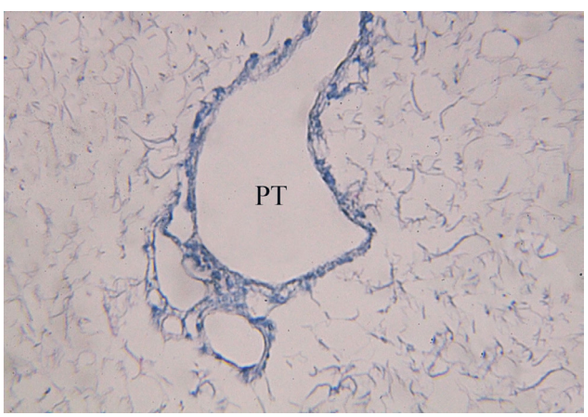

Fig. 21: A photomicrograph of a DLM of group II (decellularization group) showing condensation of collagen fibers around the portal tract (PT). (Mallory stain, x400)

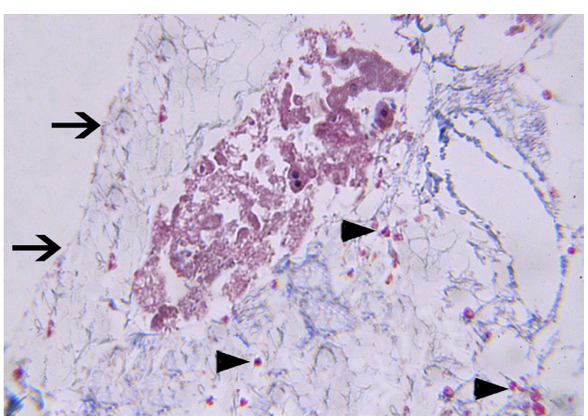

Fig. 22: A photomicrograph of a recellularized scaffold of the group III showing distribution of collagen fibers in the hepatic tissue. Condensations of collagen fibers are seen especially around large blood vessels and in the capsule of the liver (→). Large polygonal cells resembling hepatocytes are seen inside a large portal branch. Some cells infiltrate the liver matrix (►). (Mallory stain, x400)

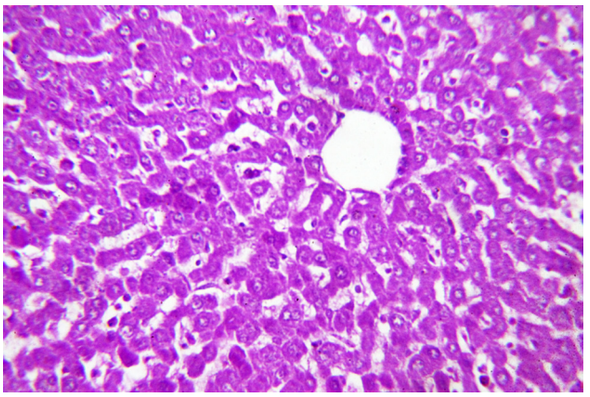

Fig. 23: A photomicrograph of an adult male albino rat liver of the control group showing central vein surrounded by radiating cords of hepatocytes that showed PAS positive reaction for glycogen. (PAS with Hx, x400)

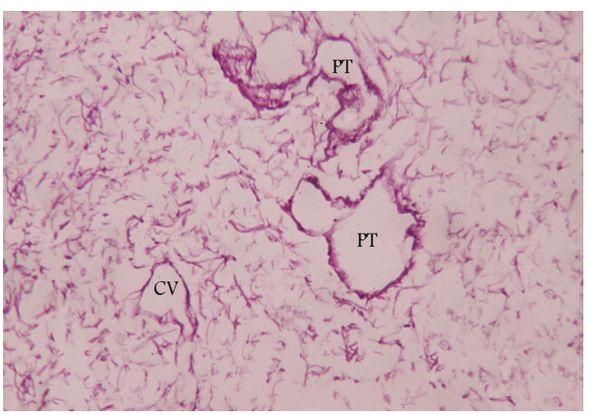

Fig. 24: A photomicrograph of a DLM of group II (decellularization group) showing central vein (CV) and portal tracts (PT) surrounded by PAS positive basement membrane with no lining cells. Radiating basement membrane of liver cords surrounding the central vein. Notice the absence of nuclear stain. (PAS with Hx, x400)

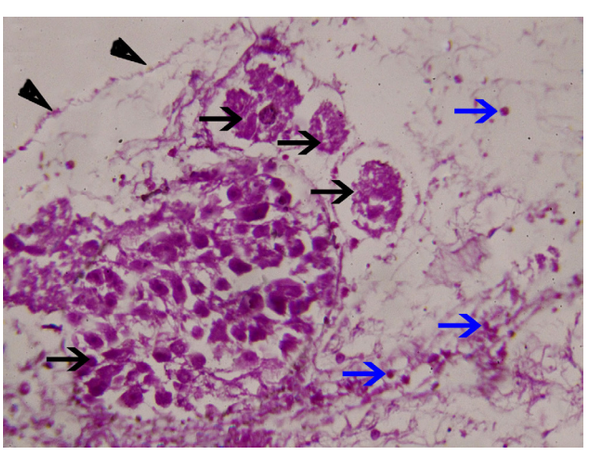

Fig. 25: A photomicrograph of a recellularized scaffold of the group III showing large polygonal PAS positive cells (black arrow) inside the portal branches. Some cells appear to infiltrate the liver matrix (blue arrow). The ECM shows PAS positive reaction especially at the capsule of liver (►). (PAS with Hx, x400)

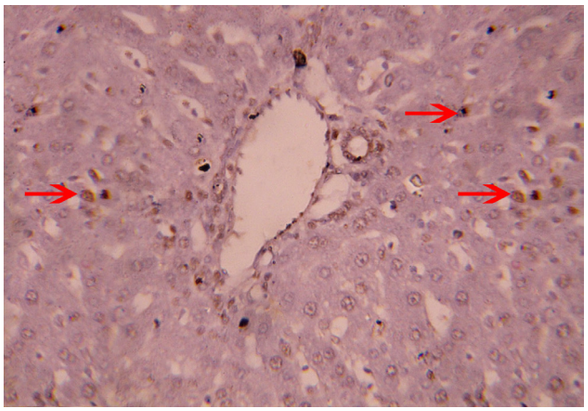

Fig. 26: A photomicrograph of an adult male albino rat liver of the control group showing portal area surrounded by radiating cords of hepatocytes. Few hepatocytes show positive intranuclear reaction for PCNA (→). (PCNA immunostaining, x400)

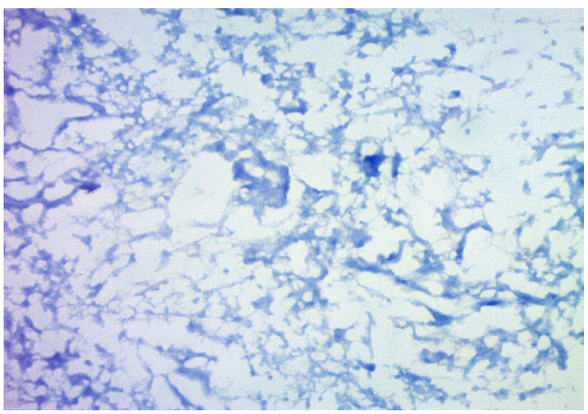

Fig. 27: A photomicrograph of a DLM of group II (decellularization group) showing only background representing general outline of liver with negative reaction for PCNA antibody. (PCNA immunostaining, x400)

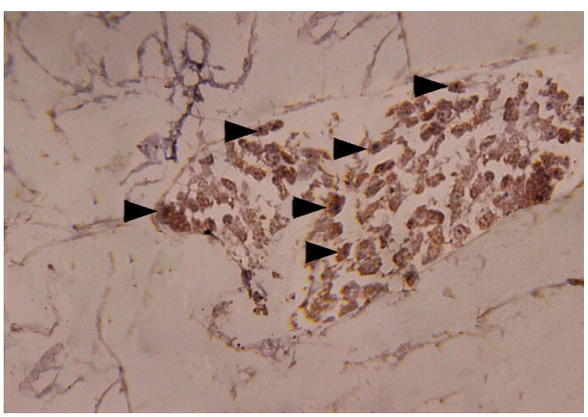

Fig. 28: A photomicrograph of a recellularized scaffold of the group III showing a PV branch filled with cells that have PCNA positive nuclear reaction (►). (PCNA immunostaining, x400)

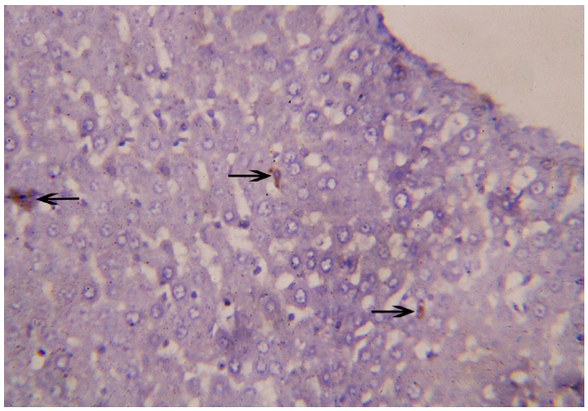

Fig. 29: A photomicrograph of an adult male albino rat liver of the control group showing portal area surrounded by radiating cords of hepatocytes. Few hepatocytes show positive cytoplasmic reaction for AFP (→). (AFP immunostaining, x400)

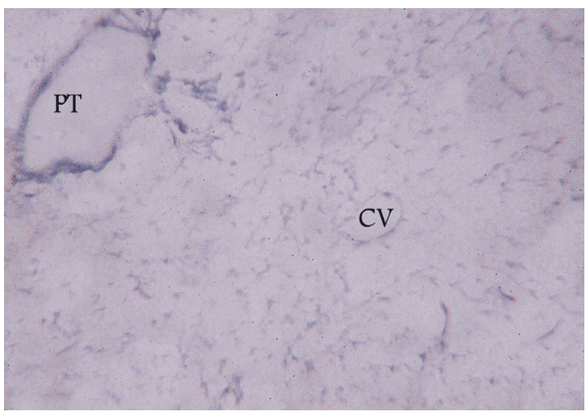

Fig. 30: A photomicrograph of a DLM of group II (decellularization group) showing the background representing general outline of liver with negative reaction for AFP antibody. (AFP immunostaining, x400)

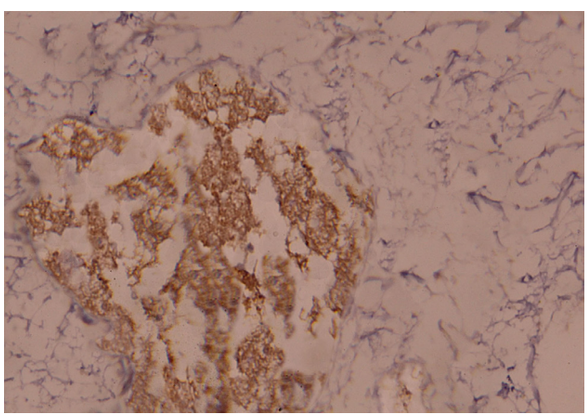

Fig. 31: A photomicrograph of a recellularized scaffold of the group III showing cells with AFP positive cytoplasmic reaction. The cells are large polygonal and present inside a portal vessel. (AFP immunostaining, x400)

Table 1: Showing mean (mean ± standard deviation) weight of livers of group II (decellularization group) before freezing/ thawing (a), after freezing/thawing (b) and after complete decellularization (c) in the present study

	Before freezing (a)	After freezing/ thawing (b)	After complete decellularization (c)
Mean Weight ± SD (gm)	15.96 ± 2.06[a]	15.53 ± 2.01[a]	5.11 ± 0.77

a significance calculated by LSD from after complete decellularization (Wt c).

Table 2: Showing the mean number of AdH cell count obtained from adult male albino rat in group III of the present study

Isolated AdH/ trial	AdHC1 (viable AdH)	AdHC2 (total AdH)	%
Mean ± SD	4.46 ± 1.87 x 10^8 cells	4.88 ± 1.92 x10^8 cells	91.39

AdHC1 viable cells, AdHC2 total number of cells, % percentage of viable cells

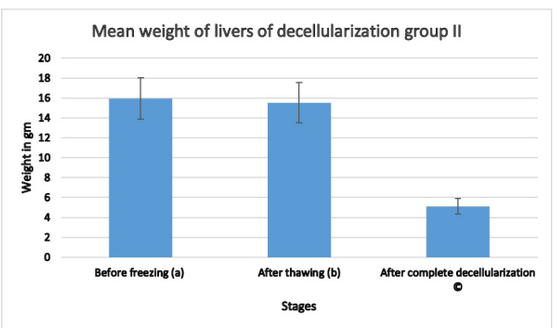

Histogram 1: Showing the mean weight of livers of group II [decellularization group] before freezing [a], after thawing [b] and after decellularization [c].

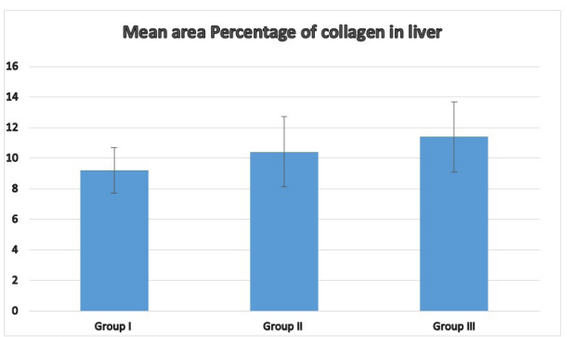

Histogram 2: showing mean area percentage of collagen fibers in livers of group I [Control group] and group II [Decellularization group] and group III [Recelularization group].

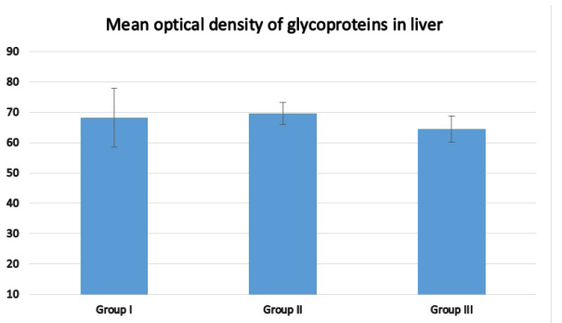

Histogram 3: showing the mean optical density of GP and PG in liver matrix in group I [control group], group II [decellularization group] and group III [Recellularization group].

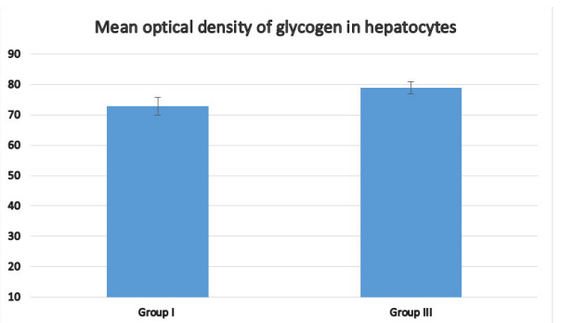

Histogram 4: showing mean optical density of glycogen in hepatocytes in group I [control group] and group III [Recellularization group].

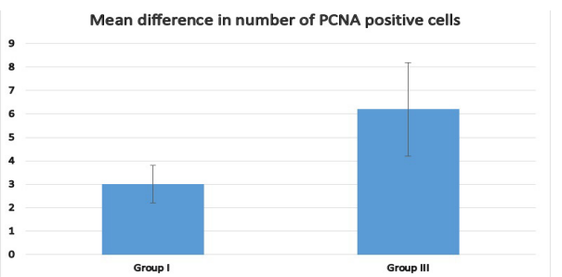

Histogram 5: showing the mean difference in number of PCNA positive cells between group I [control group] and group III [Recellularization group].

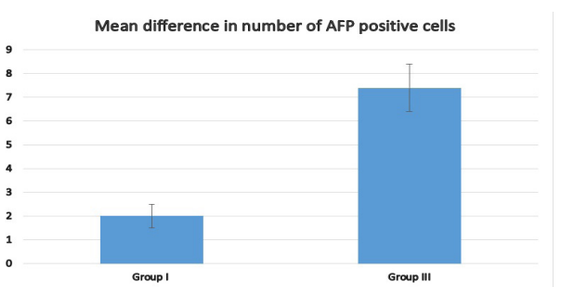

Histogram 6: Showing the mean difference in number of AFP positive cells between group I [control group] and group III [Recellularization group].

DISCUSSION

The main objectives of this study were to form a natural liver scaffold by a satisfactory decellularization technique followed by recellularization using adult male rat hepatocytes to form auxiliary hepatic tissue, and also to cultivate AdH in vitro for experimental studies and liver bioengineering.

Liver bioengineering via whole liver decellularization and recellularization using AdH was recently used since it is considered a promising modality for treatment of ESLD and for performing experimental studies. Preservation of the ECM structural proteins (e.g. collagen, glycosaminoglycans, PG, GFs) during decellularization is crucial for successful cell attachment in recellularization process[28]. Moreover, succeeding in cell attachment, proliferation, and creating a promising low cost recellularization protocol will subsequently form an auxiliary hepatic tissue. Liver recellularization is central in recent experimental studies and is growing due to the increased diversity in different fields which target the effect of different drugs (pharmaceutical testing), toxins, nutrients, and in disease modeling on the liver tissue. Therefore, creating an in-vitro model for tailored experimental studies would save money and lives of many experimental animals and could give detailed equivalent results to in *vivo* human and animal studies[6].

Regarding culture of AdH, it was well documented that liver tissue has a remarkable capacity for regeneration. Nevertheless, liver diseases are rising worldwide creating a global health burden. In ESLD, the liver loses its regenerative power, therefore, hepatocyte transplantation (HT) is considered as a good alternative treatment method. Moreover, expanding and culturing of human hepatocytes with potential proliferative capacity would treat even higher number of patients[3]. Thus, liver bioengineering is generating a new hope for hepatic patients[2].

In the present study, decellularization was performed both by physical and chemical agents. At first, physical decellularization agents (freezing and thawing) allowed initial cell disruption which facilitated the action of chemical agents. Then chemical agents (DW repeated washing, 0.5% SDS for 6-8 hrs and 1% Triton X-100 for 3-4 hrs at a rate of 6-8 ml/min) introduced through the PV was performed, thus having the benefits of allowing chemicals to reach all the cells via the native vascular tree of the liver and to wash them away via hepatic vein. Nearly similar technique was done by other researchers by perfusing different doses of SDS and Triton X-100 into PV. They mentioned that DW washed away blood remnants and cell debris while detergents as SDS and Triton X-100 disrupted cell membrane causing cell lysis and detachment from underlying ECM[12,15,18,29].

In accordance, other authors reported that perfusion of chemical detergents through the PV had the advantage of delivering chemical agents all through the liver tissue and pushing debris outside through the venous system. Besides, vascular perfusion decellularization took shorter time (hrs to few days) compared to decellularization by immersion and agitation (days to weeks). Also, vascular perfusion decellularization allowed experimentation on the whole liver tissue while conserving its gross framework (anatomy) and the microanatomy of ECM[30]. Accordingly, chemical decellularization of liver tissue in the present study was completed in hours (15 -19 hrs) to preserve both gross and histological liver structure as shown in decellularized livers of group II in this study.

Moreover, statistical analysis of different liver weights in this study showed that the mean liver weight showed nonsignificant change ($p > 0.05$) before or after the freeze/ thaw cycle (15.96 ± 2.06 gm and 15.53 ± 2.01 gm respectively). However, it showed significant decrease ($p \leq 0.05$) after complete decellularization (5.11 ± 0.77 gm) in comparison with either before or after freeze/thaw cycle. This could be attributed to apparent total loss of all parenchymatous and non-parenchymatous cells in the liver, while leaving only the ECM. In agreement, some authors discussed different decellularization techniques according to quality control criteria that includes absence of nuclear DNA material, as well as the preservation of ECM elements, micro-vascularization and mechanical properties. They found that as the decellularization protocol took longer durations (that took several days) the more the ECM was compromised[9]. This study followed the decellularization technique of some previous studies[12,15] with some modifications so that the decellularization technique would be optimized to produce DLM in short time while maintaining native structure of ECM and ensuring maximum loss of cellular components. Consequently, in group II of the present study, results of H&E sections for DLM revealed apparently complete loss of cellular and nuclear content while preserving general liver architecture. Besides, immunohistochemical staining for group II (decellularization group) showed negative reaction for both PCNA and AFP. This was due to apparent total absence of cells and lack of cellular proteins in the decellularized tissue. Similarly, other studies formed an acellular scaffold as demonstrated by H&E-stained sections. They managed to decellularize the liver leaving only minimal amount of DNA compared with cadaveric DNA[15,29].

For hepatocytes to survive in 3D decellularized scaffold, they need specific transduction between the hepatocytes and the scaffold. Thus, an optimum DLM should provide both biophysical and biochemical cues for cell proliferation. Accordingly, matrix fibers that include collagen, glycosaminoglycan, elastin, fibronectin, and laminin should be preserved in the DLM to provide strength, cell attachment sites, enhance cell migration, and tissue development[8]. Consequently, in group II of the present study, the decellularized liver sections stained by Mallory stain and PAS technique showed preserved collagen architecture together with GP, PG, and reticular fibers in the stroma of DLM. These were confirmed by

morphometric and statistical analysis of both the mean area percentage of collagen measured in Mallory-stained sections and in the mean optical density of GP and PG measured using PAS technique in the ECM of the current study. The decellularized group II showed nonsignificant difference ($p > 0.05$) when compared to either group I (control group) or to group III (recellularization group), designated adequate preservation of liver matrix in all studied groups. Accordingly, this indicated that the decellularization technique used in this study was used successfully and could be used for further studies to form a DLM for recellularization in which the reseeded hepatocytes would find attachment sites to attach and start forming new liver tissue. Moreover, this also indicated that the recellularization technique used in this study did not sever the ECM. Other researchers immunoassayed different collagen types and basement membrane components in DLM and proved that they retained similar structure to native liver. They also mentioned that increasing the dose or duration of SDS or Triton X100 would harm any protein present in the ECM[16,23,29]. Others showed that total amount of GP and PG in the ECM were well maintained after decellularization with 1% SDS and 1% Triton X100[15,31].

Regarding AdH isolation, some authors reported that AdH could be isolated after adding collagenase followed by repeated cycles of centrifugation and pellet collection for three times[32]. This method was followed in the present study in which emersion of liver pieces in collagenase for 20 min followed by three cycles of centrifugation at 1000 RPM was performed.

Some scientists reported that the lack of insulin and corticosteroids in the hepatocyte culture media leads to early aging and death in the cultured hepatocytes. This would appear as nucleus elongation, increased size and number of autophagic vacuoles inside the cell[33]. Whereas EGF is important for hepatocytes, as EGF, hepatocyte growth factor, and insulin like growth factor are vital for cell survival, differentiation and proliferation. Selective cellular receptors interact with GFs which in turn activate intracellular tyrosine kinase causing phosphorylation and activation of intracellular pathways. These pathways are vital for gene transcription and cell proliferation[34]. Furthermore, EGF is responsible for decreasing the detrimental effect of excess reactive oxygen species (ROS) in hepatocytes. ROS cause cell damage and activate apoptosis pathways. Increased levels of EGF and EGF receptors proved to protect hepatocytes from oxidative stress by increasing ROS scavenging ability and decrease ROS mediated cell death in primary hepatocytes[35]. Thus, the present study hepatocyte specific media was formed by adding insulin, corticosteroids and EGF to the traditional complete media to enhance hepatocyte viability and proliferation. Moreover, the present study compared the optical density of glycogen inside hepatocytes and showed significant increase in the mean optical density between control group (72.9 ± 3.0) and group III (78.9 ± 1.9) ($p \leq 0.05$). This indicated that hepatocytes managed to work adequately in its new scaffold. This increase might be due to the added insulin as well as the high glucose content in the HCM which sequentially increased glucose uptake and glycogen formation inside AdH[36].

This study also showed the presence of higher rate of mitosis in donor AdH that were recellularized in group III than that of group I hepatocytes by using PCNA immunostaining. The statistical analysis showed significant increase ($p \leq 0.05$) in the mean number of cells exhibiting PCNA positive reaction in their nuclei in AdH of group III (6.2 ± 2.0) compared to control group (3.0 ± 0.8), thus indicating AdH multiplication and expansion in the recellularized scaffold. Other studies proved that reseeded AdH showed peak level of PCNA at day 15[15].

Additionally, in this study, AFP immunostaining was used to prove that the recellularized AdH were proliferating hepatocytes. Statistical analysis showed significant increase ($p \leq 0.05$) in the mean number of cells exhibiting AFP positive cytoplasmic reaction in group III (7.4 ± 1.0) compared to the control group (2 ± 0.5). Practically any mature hepatocyte is able to re-express AFP if liver regeneration is induced. The AFP is considered an embryonic form of albumin and its synthesis is controlled by the formation of liver plates. When the hepatocytes form liver plate in postnatal development, AFP synthesis decreases markedly. Vice versa, loss of intercellular interaction induces AFP re-expression. Therefore, complete dissociation of adult liver tissue into single cells by collagenase will result in AFP re-expression by the second day[37].

In agreement, histological and histochemical studies of group III (recellularization group) of this study revealed that the recellularized scaffold contained aggregations of AdH that were mostly present in portal vessels in addition to the presence of few AdH in the matrix. These might be due to increased proliferation together with migration of donor AdH in the ECM respectively. Other studies showed that H&E-stained sections revealed that the majority of AdH introduced via the portal vein remained within the portal branches and only 20% successfully migrated to enter parenchyma[15,18,29].

Added to that, the present study showed that besides the proliferation of the donor AdH in the recellularized matrix in group III, the same group also showed proliferation of AdH upon cultivation in vitro. The present study showed that the primary AdH survived and exhibited 91.39% viability as indicated by trypan blue assay. Moreover, the AdH ensured their ability to proliferate and expand in HCM in vitro. They were expanded gradually till reaching confluency after 21 days from isolation. They were polygonal in shape with single or double vesicular nuclei. Also, the AdH appeared to be co-cultured with other cell types in group III on cell culture flasks, in which spindle and star shaped cells most probably fibroblast and endothelial cells with vesicular nucleus and elongated cell processes were noticed extending between the cultured

AdH. In agreement, some studies showed that co-culturing technique enhanced hepatocyte proliferation and stabilized cell culture. Hepatocyte/fibroblast/endothelial cell triculture elucidated specific to specific cellular mechanisms which were important for physiological as well as pathological processes. Co-culturing technique created a relevant liver models used for experiments as in drug metabolism and toxicity pathways[38].

Finally, some studies noted that culturing and expanding of AdHs is important as they can be used as a new treatment modality by their transplantation to hepatic patients. Moreover, several advantages of HT over liver transplantation as being less expensive and less invasive surgical procedure and can be repeated if required. The HT procedure requires a small percentage of AdH isolated from one donor liver and these cells can be cultured and multiplied, and most importantly several patients can be treated from one donor liver. Added to that, cryopreservation of the isolated cells is always available for use. Moreover, the native liver remains in place as a backup that can allow potential regeneration in patients with acute liver failure[39]. Accordingly, it is accepted to treat patients with acute liver failure with HT in order to allow self-regeneration till recovery. It is estimated that only 10 – 15 % of liver cell mass is needed in these patients, thus many cases with acute liver failure can be recovered clinically simultaneously using HT obtained from one adult donor liver. However, still randomized controlled trials are needed to prove its efficiency[40].

CONCLUSION AND RECOMMENDATION

It is concluded that the present study managed to present efficient decellularization for adult rat livers forming a natural scaffold that accommodated proliferating AdH for several days while preserving integrity of most of the structural components of the ECM. Besides, this study managed to cultivate and proliferate AdH in vitro till confluency for 21 days. Accordingly, the techniques used in this study represented advancement in the understanding of bio-engineered livers.

It is recommended that more work is needed to examine the functional effectiveness of the formed recellularized liver scaffolds both in *vivo* and in vitro.

CONFLICT OF INTERESTS

There are no conflicts of interest.

REFERENCES

1. Gomaa A, Allam N, Elsharkawy A, El Kassas M, Waked I. Hepatitis C infection in Egypt: prevalence, impact and management strategies. Hepat Med. 2017;9:17-25. doi:10.2147/HMER.S113681
2. Misra AC, Eckhoff D. The development of artificial livers. Curr Opin Organ Transplant. 2021;26(5).
3. Haep N, Florentino RM, Squires JE, Bell A, Soto-Gutierrez A. The Inside-Out of End-Stage Liver Disease: Hepatocytes are the Keystone. Semin Liver Dis. 2021;41(2):213-224. doi:10.1055/s-0041-1725023
4. Kwak KA, Lee SP, Yang JY, Park YS. Current perspectives regarding stem cell-based therapy for Alzheimer?s disease. Stem Cells Int. 2018;2018:21-23. doi:10.1155/2018/6392986
5. Hindley CJ, Cordero-espinoza L, Huch M. Organoids from adult liver and pancreas : Stem cell biology and biomedical utility. Dev Biol. 2016;420(2):251-261. doi:10.1016/j.ydbio.2016.06.039
6. Dzobo K, Shirley K, Motaung CM, Adesida A. Recent Trends in Decellularized Extracellular Matrix Bioinks for 3D Printing : An Updated Review. Int J Mol Sci. 2019;20(4628):1-28.
7. Park KM, Hussein KH, Hong SH, *et al*. Decellularized Liver Extracellular Matrix as Promising Tools for Transplantable Bioengineered Liver Promotes Hepatic Lineage Commitments of Induced Pluripotent Stem Cells. Tissue Eng - Part A. 2016;22(5-6):449-460. doi:10.1089/ten.tea.2015.0313
8. Padhi A, Nain AS. ECM in Differentiation: A Review of Matrix Structure, Composition and Mechanical Properties. Ann Biomed Eng. 2020;48(3):1071-1089. doi:10.1007/s10439-019-02337-7
9. Rossi EA, Quintanilha LF, Kymie C, Nonaka V, Solano B, Souza DF. Review Article Advances in Hepatic Tissue Bioengineering with Decellularized Liver Bioscaffold. 2019;2019.
10. Butter A, Aliyev K, Hillebrandt K, *et al*. Evolution of graft morphology and function after recellularization of decellularized rat livers. 2018;(June 2017):807-816. doi:10.1002/term.2383
11. Maghsoudlou P, Georgiades F, Smith H, *et al*. Optimization of Liver Decellularization Maintains Extracellular Matrix Micro-Architecture and Composition Predisposing to Effective Cell Seeding. PLoS One. 2016;11(5):e0155324. doi:10.1371/journal.pone.0155324
12. Chen Y, Geerts S, Jaramillo M, Uygun BE. Preparation of Decellularized Liver Scaffolds and Recellularized Liver Grafts. Methods Mol Biol. 2018;1577(August 2017):255-270. doi:10.1007/7651_2017_56
13. Ogoke O, Oluwole J, Parashurama N. Bioengineering considerations in liver regenerative medicine. 2017:1-16. doi:10.1186/s13036-017-0081-4
14. Lorenzo SB De, Nyberg L. Recent Advances in Decellularization and Recellularization for Tissue-Engineered Liver Grafts. J Micromech Microeng. 2017;55901:203-214. doi:10.1159/000452761
15. Robertson MJ, Soibam B, O'Leary JG, Sampaio LC, Taylor DA. Recellularization of rat liver: An in vitro model for assessing human drug metabolism and liver biology. PLoS One. 2018;13(1):1-23. doi:10.1371/journal.pone.0191892

16. Ghiringhelli M, Zenobi A, Brizzola S, *et al*. Simple and quick method to obtain a decellularized, functional liver bioscaffold. In: Methods in Molecular Biology. Vol 1577. ; 2018:283-292. doi:10.1007/7651_2017_97

17. Flecknell P. Laboratory Animal Anaesthesia.; 2009. doi:10.1016/B978-0-12-369376-1.X0001-9

18. Ogiso S, Yasuchika K, Fukumitsu K, *et al*. Efficient recellularisation of decellularised whole-liver grafts using biliary tree and foetal hepatocytes. Sci Rep. 2016;6(October):1-10. doi:10.1038/srep35887

19. Kegel V, Deharde D, Pfeiffer E, Zeilinger K, Seehofer D, Damm G. Protocol for isolation of primary human hepatocytes and corresponding major populations of non-parenchymal liver cells. J Vis Exp. 2016;2016(109):1-10. doi:10.3791/53069

20. Deshmukh A. Rat hepatocytes maintained at a refrigerating temperature for rat hepatocytes maintained at a refrigerating temperature for one week exhibit a high. CIBTech J Biotechnol. 2012;1(July 2012):64-68.

21. Williams GM, Bermudez E, Scaramuzzino D, al wet. Rat hepatocyte primary cell cultures iii . Improved Dissociation and Attachment Techniques and the Enhancement of Survival by Culture Medium The conditions for obtaining representative , adult rat hepatocyte primary cell culture. In Vitro. 1977;13(12).

22. Aday S, Hasirci N, Gurhan ID. A cost-effective and simple culture method for primary hepatocytes. Animal Cells Syst (Seoul). 2011;15(1):19-27. doi:1.1080/19768354.2011.555140

23. Shirakigawa N, Ijima H. Decellularization of liver and organogenesis in rats. In: Methods in Molecular Biology. Vol 1577. ; 2018:271-281. doi:10.1007/7651_2017_63

24. Mirmalek-Sani S-H, Sullivan DC, Zimmerman C, Shupe TD, Petersen BE. Immunogenicity of Decellularized Porcine Liver for Bioengineered Hepatic Tissue. Am J Pathol. 2013;183(2):558-565. doi:https://doi.org/10.1016/j.ajpath.2013.05.002

25. Mattei G, Magliaro C, Pirone A, Ahluwalia A. Decellularized Human Liver Is Too Heterogeneous for Designing a Generic Extracellular Matrix Mimic Hepatic Scaffold. Artif Organs. 2017;41(12):E347-E355. doi:10.1111/aor.12925

26. Lee H, Han W, Kim H, *et al*. Development of Liver Decellularized Extracellular Matrix Bioink for Three-Dimensional Cell Printing-Based Liver Tissue Engineering. Biomacromolecules. 2017;18(4):1229-1237. doi:10.1021/acs.biomac.6b01908

27. Zheng X, Liu W, Liu F, *et al*. Decellularized matrix of human fatty liver used for three-dimensional culture of hepatocellular carcinoma cells. Nan Fang Yi Ke Da Xue Xue Bao. 2019;39(8):930-936. doi:10.12122/j.issn.1673-4254.2019.08.09

28. Yaghoubi A, Azarpira N, Karbalay-Doust S, Daneshi S, Vojdani Z, Talaei-Khozani T. Prednisolone and mesenchymal stem cell preloading protect liver cell migration and mitigate extracellular matrix modification in transplanted decellularized rat liver. Stem Cell Res Ther. 2022;13(1):36. doi:10.1186/s13287-022-02711-8

29. Uygun BE, Soto-Gutierrez A, Yagi H, *et al*. Organ reengineering through development of a transplantable recellularized liver graft using decellularized liver matrix. Nat Med. 2010;16(7):814-820. doi:10.1038/nm.2170

30. Mazza G, Al-Akkad W, Rombouts K, Pinzani M. Liver tissue engineering: From implantable tissue to whole organ engineering. Hepatol Commun. 2018;2(2):131-141. doi:10.1002/hep4.1136

31. Nobakht Lahrood F, Saheli M, Farzaneh Z, *et al*. Generation of transplantable three-dimensional hepatic-patch to improve the functionality of hepatic cells in vitro and in *vivo*. Stem Cells Dev. 2020;29(5):301-313. doi:10.1089/scd.2019.0130

32. Horner R, Gassner JGM V, Kluge M, *et al*. Impact of Percoll purification on isolation of primary human hepatocytes. Sci Rep. 2019;9(1):6542. doi:10.1038/s41598-019-43042-8

33. Aravinthan A, Challis B, Shannon N, Hoare M, Heaney J, Alexander GJM. Selective insulin resistance in hepatocyte senescence. Exp Cell Res. 2015;331(1):38-45. doi:https://doi.org/10.1016/j.yexcr.2014.09.025

34. Musallam L, Éthier C, Haddad PS, Bilodeau M. Role of EGF receptor tyrosine kinase activity in antiapoptotic effect of EGF on mouse hepatocytes. Am J Physiol - Gastrointest Liver Physiol. 2001;280(6 43-6):1360-1369. doi:10.1152/ajpgi.2001.280.6.g1360

35. Kim M-J, Choi W-G, Ahn K-J, Chae IG, Yu R, Back SH. Reduced EGFR Level in eIF2α Phosphorylation-Deficient Hepatocytes Is Responsible for Susceptibility to Oxidative Stress. Mol Cells. 2020;43(3):264-275. doi:10.14348/molcells.2020.2197

36. Nagarajan SR, Paul-Heng M, Krycer JR, Fazakerley DJ, Sharland AF, Hoy XAJ. Lipid and glucose metabolism in hepatocyte cell lines and primary mouse hepatocytes: A comprehensive resource for in vitro studies of hepatic metabolism. Am J Physiol - Endocrinol Metab. 2019;316(4):E578-E589. doi:10.1152/ajpendo.00365.2018

37. Lorvellec M, Scottoni F, Crowley C, *et al*. Mouse decellularised liver scaffold improves human embryonic and induced pluripotent stem cells differentiation into hepatocyte-like cells. PLoS One. 2017;12(12):1-15. doi:10.1371/journal.pone.0189586

38. Ware BR, Durham MJ, Monckton CP, Khetani SR. A Cell Culture Platform to Maintain Long-term Phenotype of Primary Human Hepatocytes and Endothelial Cells. Cmgh. 2018;5(3):187-207. doi:10.1016/j.jcmgh.2017.11.007

39. Iansante V, Mitry RR, Filippi C, Fitzpatrick E, Dhawan A. Human hepatocyte transplantation for liver disease: Current status and future perspectives. Pediatr Res. 2018;83(1-2):232-240. doi:10.1038/pr.2017.284

40. Cardoso LMDF, Moreira LFP, Pinto MA, Henriques-Pons A, Alves LA. Domino Hepatocyte Transplantation: A Therapeutic Alternative for the Treatment of Acute Liver Failure. Can J Gastroenterol Hepatol. 2018;2018. doi:10.1155/2018/2593745

الملخص العربى

الهندسه الطبيه الحيويه لنسيج الكبد: نزع الخلايا من النسيج واعاده زراعته. دراسه هستولوجيه وهستوكيميائيه مناعيه

شيماء فطين خضر، نجوى قسطندى قلينى، نفرت فريد عبد السلام

قسم الهستولوجيا و بيولوجيا الخليه، كليه الطب، جامعه عين شمس، القاهره، مصر

المقدمه: تتزايد الحاجه الى زراعه الكبد بسبب زياده المصابين بأمراض الكبد المستعصيه. كما إن تكوين عُضيات الكبد يؤدى إلى إنشاء نموذج إصطناعي للكبد في المختبر مصمم خصيصا للدراسات التجريبية على الأدويه و تأثيرها السام على خلايا الكبد.

الهدف: صممت هذه الدراسة للحصول على دعامه كبد طبيعية منزوعة الخلايا ثم زراعتها بخلايا الكبد البالغه لتكوين عُضيات الكبد. إلى جانب زراعة خلايا الكبد البالغة في المختبر في قوارير الإستزراع لإستخدامها فى التجارب و لإنشاء نموذج إصطناعي للكبد.

المواد و الطرق: المجموعة الأولى (المجموعة الضابطة): تتكون من ١٠ جرذا بالغاً. المجموعة الثانية (مجموعة إزالة الخلايا): تتكون من ١٠ جرذا بالغاً تم نزع الخلايا من كبدها لتكون دعامه كبديه منزوعه الخلايا. المجموعة الثالثة (مجموعة إعادة الخلايا الكبدية): تتكون من ٢٠ جرذًا بالغاً حيث تم اعتبار ١٠ جرذا بالغاً مانحة لـخلايا الكبد ليتم زرعتها فى قوارير الإستزراع إلى جانب ١٠ جرذا بالغا تم نزع الخلايا من كبدها ثم زراعتها بجزء أخر من خلايا الكبد لتكوين دعامه كبديه. بعد إنتهاء التجربه، تمت معالجة الكبد (المجموعه الضابطه، مجموعة إزالة الخلايا، ومجموعة إعادة الخلايا الكبدية) بإستخدام التقنيات النسيجية والكيميائية النسيجية والكيميائية المناعية. كما تم إجراء دراسات مورفومترية وإحصائية.

النتائج: بالعين المجرده ظهر الكبد منزوع الخلايا شبه شفاف. فى حين أظهر فحص المقاطع المصبوغه للمجموعة الثانية (مجموعة إزالة الخلايا) فقدًا كليًا للمواد الخلوية والنووية مع الحفاظ على محتوى الكولاجين والبروتين السكري في الدعامه الحيويه. كما أظهرت خلايا الكبد المزروعة في قوارير الأستزراع زيادة تدريجية في العدد حتى نسبه ٩٠-٩٥ من الالتقاء في اليوم ٢١. ظهرت خلايا الكبد كخلايا متعددة الأضلاع مع سيتوبلازم حُبيبي مع وجود خلايا أخرى مزروعه فى طبق الاستزراع. في حين أظهر فحص المقاطع المصبوغه للمجموعة الثالثة (مجموعة إعادة الخلايا) تجمعات من خلايا الكبد في الفروع البابيه مع الحفاظ على الهيكل العام للكبد. ظهرت خلايا الكبد متعدده الاضلاع مع سيتوبلازم حُبيبي إيجابى التفاعل لصبغه PAS . كما ظهر زيادة كبيرة في متوسط عدد الخلايا التي تظهر تفاعلًا إيجابيًا لبروتين تكاثر نواة الخلية PCNA وبروتين ألفا الجنيني AFP.

الاستنتاج: تم زراعة خلايا الكبد البالغة في قوارير الإستزراع حتى نسبه ٩٥٪ من الإلتقاء. كما تمكنت الدراسه من إزالة الخلايا بكفاءة من كبد الجرذان لكى تشكل سقالة طبيعية يمكنها أن تستوعب خلايا الكبد البالغه بالإضافة إلى تحفيز تكاثرها مع الحفاظ على سلامة معظم المكونات الهيكلية للنسيج اللاخلوى. هذا النموذج الإصطناعي للكبد و خلايا الكبد المزروعه فى قوارير الإستنبات يمكن إستخدامهم للأختبارات الصيدلانيه على نماذج الكبد ويمكن أن يكونوا أملًا جديدًا للمرضى الذين يعانون من أمراض الكبد.